Physics Letters B 788 (2019) 225–230

Contents lists available at ScienceDirect

Physics Letters B

www.elsevier.com/locate/physletb

The concept of nuclear photon strength functions: A model-independent approach via $(\vec{\gamma}, \gamma'\gamma'')$ reactions

J. Isaak [a,b,c,*], D. Savran [b], B. Löher [a,b], T. Beck [a], M. Bhike [d], U. Gayer [a], Krishichayan [d], N. Pietralla [a], M. Scheck [e], W. Tornow [d], V. Werner [a], A. Zilges [f], M. Zweidinger [a]

[a] Institut für Kernphysik, Technische Universität Darmstadt, Schlossgartenstr. 9, 64289 Darmstadt, Germany
[b] GSI Helmholtzzentrum für Schwerionenforschung GmbH, Planckstr. 1, 64291 Darmstadt, Germany
[c] Research Center for Nuclear Physics, Osaka University, 10-1 Mihogaoka, Ibaraki, Osaka 567-0047, Japan
[d] Department of Physics, Duke University and Triangle Universities Nuclear Laboratory, Durham, NC 27708-0308, USA
[e] School of Computing, Engineering, and Physical Sciences, University of the West of Scotland, Paisley, PA1 2BE, UK
[f] Universität zu Köln, Institut für Kernphysik, Zülpicher Str. 77, 50937 Köln, Germany

ARTICLE INFO

Article history:
Received 19 July 2018
Received in revised form 5 November 2018
Accepted 19 November 2018
Available online 22 November 2018
Editor: W. Haxton

Keywords:
Photon strength function
Statistical model
γ-ray spectroscopy
γ–γ coincidence experiments

ABSTRACT

Most theoretical approaches used in nuclear astrophysics to model the nucleosynthesis of heavy elements incorporate the so-called statistical model in order to describe the excitation and decay properties of atomic nuclei. One of the basic assumptions of this model is the validity of the Brink–Axel hypothesis and the related concept of so-called photon strength functions to describe γ-ray transition probabilities. We present a novel experimental approach that allows for the first time to experimentally determine the photon strength function simultaneously in two independent ways by a unique combination of quasi-monochromatic photon beams and a newly implemented γ–γ coincidence setup. This technique does not assume a priori the validity of the Brink–Axel hypothesis and sets a benchmark in terms of the detection sensitivity for measuring decay properties of photo-excited states below the neutron separation energy. The data for the spherical off-shell nucleus ^{128}Te were obtained for γ-ray beam-energy settings between 3 MeV and 9 MeV in steps of 130 keV for the lower beam energies and in steps of up to 280 keV for the highest beam settings. We present a quantitative analysis on the consistency of the derived photon strength function with the Brink–Axel hypothesis. The data clearly demonstrate a discrepancy of up to a factor of two between the photon strength functions extracted from the photoabsorption and photon emission process, respectively. In addition, we observe that the photon strength functions are not independent of the excitation energy, as usually assumed. Thus, we conclude, that the Brink–Axel hypothesis is not strictly fulfilled in the excitation-energy region below the neutron separation threshold ($S_n = 8.78$ MeV) for the studied case of ^{128}Te.

1. Introduction

Currently, the modeling of a significant part of the synthesis of the elements in the universe is built on basic assumptions in the description of nuclear properties, such as the so-called Brink–Axel (BA) hypothesis [1,2]. Electromagnetic decay processes, in particular so-called γ radiation, are important ingredients for astrophysical models. The BA hypothesis assumes that the average electromagnetic decay rate merely depends on the transition energy of the emitted γ radiation, but it does not depend on either the absolute excitation energy of the nucleus or the specific properties of the nuclear states involved. This hypothesis is used as the basis of the treatment of γ-ray transition probabilities in the concept of photon strength functions (PSF). It is widely applied in calculations of stellar reaction rates and the modeling of nucleosynthesis of the majority of the chemical elements heavier than iron (e.g., Refs. [3–5] and references therein). In addition, it is used in combination with the statistical model (SM), that was formulated and introduced by Hauser and Feshbach [6] and has impacts on other applications that make use of reaction-model codes like EMPIRE [7] and TALYS [8] (which incorporate the statistical model) such as the design of the next-generation nuclear power plants [9] and the transmutation of nuclear waste [10,11].

* Corresponding author.
E-mail address: jisaak@ikp.tu-darmstadt.de (J. Isaak).

https://doi.org/10.1016/j.physletb.2018.11.038

The concept of the PSF relies on the fact that at high excitation energies the nuclear level densities (NLD) of atomic nuclei is reasonably high to allow for a sufficiently precise averaged treatment of the excitation spectrum and the nuclear decay properties. The PSF describes the average probability to emit or absorb γ radiation with a given γ-ray energy (E_γ). Therefore, it is also directly connected to the photoabsorption cross section σ_γ. For heavy spherical nuclei (such as ^{128}Te, which we consider here) the by far most dominant component in the photoabsorption cross section σ_γ is the electric dipole ($E1$) radiation, which at high excitation energies is described by the well-known isovector Giant Dipole Resonance (IVGDR) [12]. At intermediate energies, on the low-energy tail of the IVGDR an additional structure, the Pygmy Dipole Resonance (PDR), has been reported in the $E1$ response of the ground state of numerous nuclei [13]. While in some reactions a similar structure was observed in the $E1$ part of the PSF derived from decay properties, there are experimental indications [14–16], that the specific structure of the PDR is breaking the concept of a single PSF for all excitation energies and final states.

The SM and the BA hypothesis are well established in the energy regime of the giant resonances with excitation energies in the 10 to 20 MeV energy range (see Refs. [12,17] and references therein). In contrast, its reliability at lower excitation energies, especially in the region of the particle separation thresholds, is still a matter of ongoing theoretical (e.g., Refs. [18–22] and references therein) and experimental research (e.g., Refs. [16,23–33] and references therein), respectively. There have been many trials to study and test the assumptions of the BA hypothesis. Experimental studies were performed, amongst others, through photon-scattering measurements (e.g., [15,30,34–36]), the analysis of γ-ray spectra following particle-induced reactions (see, e.g., Refs. [28,29,31,33,37–39]), as well as from two-step γ cascades in compound nuclei (e.g., [27,40,41]).

Recently, the comparison of experimental studies using inelastic proton scattering at very forward angles to data from photon-scattering experiments and (^{3}He, ^{3}He'γ) measurements support the assumptions of the BA hypothesis in the case of the nucleus ^{96}Mo [33]. However, the statistical precision of the data in Ref. [33] does not allow to draw final conclusions and that statement remains qualitative.

In this manuscript we present a new experimental technique that allows for the first time to derive the PSF from excitations of the ground state to excited states as well as from the subsequent decay of these excited states in a single experiment in two model-independent ways. This allows to test the consequence of the BA hypothesis that the photoabsorption and the photon emission process can be treated equivalently and, thus, the PSFs for both processes are the same. We present a quantitative analysis on the consistency of the derived PSF, which is only possible due to the high accuracy of our experimental data. Our experimental technique exploits the combination of nuclear resonance fluorescence (NRF) experiments [42] using quasi-monochromatic photon beams and a high-efficiency γ-ray detection setup, which allows to perform γ–γ coincidence spectroscopy. This unique combination allows for the experimental extraction of the PSF in two independent ways as outlined below.

2. Experimental approach

The first approach to extract the PSF from the present experimental data utilizes the connection to the photoabsorption cross section σ_γ as mentioned before. In order to measure the full photoabsorption cross section the monochromatic character of the photon beam plays an important role. Subsequent to the photoabsorption process, it allows to determine in a model-independent way the so-called "elastic" part, that represents the fraction decaying directly back to the ground state. Due to the vanishing contribution from non-resonant γ-ray background at the excitation energy, the complete ground-state transition intensity including the unresolved strength (sometimes considered as background in a state-to-state analysis) hidden below resolved transitions is extracted by a detector response deconvolution procedure [43,44]. The "inelastic" part is composed of all deexcitations that decay via intermediate excited levels. The selectivity of the NRF reaction for populating $J = 1$ states in an even–even nucleus like ^{128}Te and the subsequent dominant decay via dipole and quadrupole transitions leads to the assumption, that most of the cascading events will decay via the first few excited states [45]. Hence, these excited states serve as a kind of funnel collecting most of the "inelastic" transitions. Therefore, their observed total transition intensities serve as an estimation of the "inelastic" contribution [15,36,45–47]. The sum of the "elastic" and "inelastic" parts results in the full photoabsorption cross section at a given excitation energy region that is defined by the width of the incoming quasi-monochromatic photon beam. In the following, the PSF extracted from σ_γ is denoted as $f^\sigma(E_\gamma)$.

The second approach is making use of the fact that the PSF is linked to the average decay intensity of the excited states in a given excitation energy interval to lower-lying excited levels of the nucleus. This approach has been used before to determine the shape of the PSF in a particle-induced reaction [29]. However, only the NRF reaction as used in the present study allows for a clear identification of the radiation character of the transitions, and the spin of the excited states via the polarization of the photon beam [44], while simultaneously providing $f^\sigma(E_\gamma)$ from the photoabsorption cross section. In the following, the quantity σ_{ik} denotes the cross section to excite the nucleus into the energy region E_i and the subsequent decay to the final excited state k at energy E_k. Then the ratio of the PSF at two decay γ-ray transition energies $E_i - E_k$ and $E_i - E_j$ is proportional to the ratio of the decay intensities σ_{ik} and σ_{ij} to the two excited states k and j, respectively:

$$\frac{\sigma_{ik}}{\sigma_{ij}} = \frac{f(E_i - E_k)}{f(E_i - E_j)} \cdot \frac{(E_i - E_j)^3}{(E_i - E_k)^3} \quad (k, j) \neq 0, \tag{1}$$

where the condition $(k, j) \neq 0$ (excluding the decay channel back to the ground state) is required to adapt the method of extracting the PSF from relative decay intensities outlined in Ref. [29] to the NRF reaction. It is assumed in Eq. (1) that dipole transitions are the dominant component of the integrated decay intensities for a given excitation energy. Therefore, the measurement of primary transitions to different excited states for a given excitation energy region (defined by the γ-ray beam energy) allows to extract ratios of the PSF for different γ-ray energy combinations. The high detection sensitivity of γ–γ coincidence spectroscopy is crucial to observe these direct transitions to excited levels and to determine σ_{ik} even for very weak decay branches, which was realized for NRF measurements by the γ^3 setup [47,48]. Scanning the nucleus in closely-meshed intervals by using different beam energies provides multiple ratios of the PSF over a large range of γ-ray energies. If the BA hypothesis holds and a single PSF, independent of the final state and the excitation energy, can be used to describe the γ-decay properties of the nucleus, all these data sets will be consistent with each other for PSF values at the same γ-ray energies and, consequently, the overall shape of the PSF can be extracted. Therefore, this method allows not only to extract the PSF, but also to test, if the BA hypothesis is valid in the present case. In the following, the PSF extracted from the observed primary transitions

is denoted as $f^{p}_{exp}(E_\gamma)$ and $f^{p}_{sim}(E_\gamma)$ (superscript $p \equiv$ primary) for the analysis of the experimental and simulated data, respectively. Note that by construction, the PSF is determined only to an overall scaling factor, since it is derived via ratios of the PSF.

3. Experimental details

In this letter, data from $(\vec{\gamma}, \gamma'\gamma'')$ measurements on ^{128}Te are presented. The experiments were performed at the High Intensity γ-ray Source (HIγS) [49] at Triangle Universities Nuclear Laboratory, Durham, NC, USA. Fully linearly polarized γ-ray beams are generated by laser Compton backscattering (LCB) of intracavity free-electron-laser photons off relativistic electrons. The typical full width at half maximum (FWHM) of the LCB beams spectral distribution is about $\Delta E/E \sim 3$–4% with intensities of about $10^7 \gamma/s$ on target. This allows the study of photoexcited nuclear levels in a well-defined excitation-energy range defined by the beam energy and width, respectively.

The γ-ray spectroscopy was performed with the γ–γ coincidence setup γ^3 [48]. The γ^3 setup consists of High Purity Germanium (HPGe) detectors and cerium-doped Lanthanum Bromide ($LaBr_3$:Ce) scintillators positioned in a close geometry around the target position. For a detailed description of the experimental setup and technical features, see Ref. [48]. The combination of LCB γ-ray beams with the γ–γ coincidence method allows to investigate in detail decay channels other than to the ground state in real-photon scattering experiments, which is the key feature in the present analysis.

The target consisted of 2913 mg isotopically-enriched (99.8%) ^{128}Te in metallic form. In total, 30 different LCB γ-ray beam settings between 3 MeV and 9 MeV mean energy were used to scan the excitation spectrum in 130 keV steps for the lower energies and steps of up to 280 keV for the highest beam-energy settings. The low-energy threshold in the measurements was set to $\sim$ 600 keV to allow γ–γ coincidence spectroscopy starting from the first excited 2^+ state at 743 keV while cutting off as much as possible of the low-energy background γ-rays. The focus in the following section is set on the analysis of the γ–γ coincidence data using the $LaBr_3$:Ce scintillators.

As a typical example, Fig. 1 shows summed coincidence spectra obtained with the $LaBr_3$:Ce detectors for a beam energy of $E_{beam} =$ 8 MeV. The dashed lines illustrate the beam profile shifted by the excitation energy of the populated low-lying excited states indicating the region of interest for the extraction of the averaged population intensities. The spectrum in Fig. 1.a) is obtained by gating on the energy of the $2^+_1 \rightarrow 0^+_1$ transition ($E_\gamma = 743$ keV), subtracting contributions from random coincidences and correcting for the detector response. The uncertainties of the detector response correction is given by the shaded bands. A detailed description on the various analysis steps can be found in Refs. [43,44,47]. The resulting spectrum contains full-energy events, only. The well-separated peak at the high-energy end of the spectrum can be assigned to the direct population of the 2^+_1 state at $E_{2^+_1} = 743$ keV from excited levels at $E_{beam} = 8$ MeV corresponding to $E_\gamma = 7.26$ MeV. Events below 7 MeV are attributed to transitions to other excited states, which decay via the 2^+_1 state and, thus, are measured in coincidence to the $2^+_1 \rightarrow 0^+_1$ transition as well. However, it is difficult to separate those individual transitions due to the spectral width of the photon beam of FWHM roughly 300 keV.

In some cases it is not possible to apply isolated gates on individual transitions, such as the $2^+_3 \rightarrow 2^+_1$ transition, as the γ-rays stemming from the $0^+_2 \rightarrow 2^+_1$ transition are too close in energy ($E_{2^+_3 \rightarrow 2^+_1} = 1225$ keV, $E_{0^+_2 \rightarrow 2^+_1} = 1235$ keV) to be resolved with the $LaBr_3$:Ce detectors. However, if the ansatz of the SM is valid, the direct population of low-lying levels is independent of the associated angular-momentum quantum number and a function of E_γ and of the γ-ray multipolarity, only.

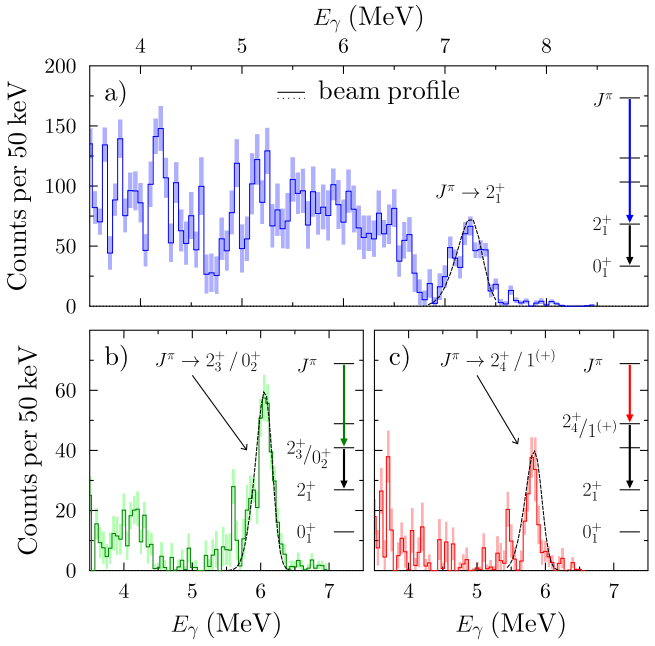

Fig. 1. Typical experimental γ–γ coincidence spectra for ^{128}Te using a photon-beam energy of $E_{beam} = 8$ MeV. Gating on different transitions in ^{128}Te, such as **a**) $2^+_1 \rightarrow 0^+_1$, **b**) $2^+_3/0^+_2 \rightarrow 2^+_1$ and **c**) $2^+_4/1^{(+)} \rightarrow 2^+_1$ results in the γ-ray spectra displayed. The uncertainties of the detector response deconvolution procedure are shown as colored uncertainty bands. The dashed lines indicate the incoming beam profile shifted by the corresponding excitation energy of the populated low-lying levels. For details see text.

Two additional examples are given in Figs. 1.b) and c) for the direct population of the $2^+_3/0^+_2$ and $2^+_4/1^{(+)}$ levels, respectively. Again, the high-energy peaks observed in the spectra correspond to primary transitions to the $2^+_3/0^+_2$ and $2^+_4/1^{(+)}$ level, respectively. This procedure is applied for primary transitions populating levels up to the 2^+_8 state in ^{128}Te for excitation energies above 6.4 MeV.

The spectra displayed in Fig. 1 strongly highlight the sensitivity obtained using the γ^3 setup at HIγS by combining γ–γ coincidence measurements with quasi-monochromatic photon beams [47,48]. This provides a new benchmark for the sensitivity of observing weak transitions to low-lying excited states compared to the capability of standard NRF experiments. In addition, the polarized character of the photon beam allows to assign a dominant $E1$ character for primary γ-ray transitions to the 2^+_1 state conducting a multipole decomposition analysis [44], while the statistics are not sufficient to unambiguously assign the transition character to other low-lying 2^+ levels. However, in the presented work the different dipole components of the PSF are not particularly distinguished. Instead, the sum of both dipole contributions ($E1$ and $M1$) is determined.

4. Results and discussion

The analysis presented in the previous section was performed for all photon-beam settings. For each beam energy relative intensities σ_{ik}/σ_{ij} (see Eq. 1) for the direct population of low-lying levels were determined. These ratios are used to extract values of $f^{p}_{exp}(E_\gamma)$ relative to the PSF value $f^{p}_{exp}(E_{\gamma_0})$ at a chosen reference energy E_{γ_0}. The results of all measurements are summarized in Fig. 2.a) as black dots after scaling the individual data sets obtained at different beam energies in order to minimize fluctuations

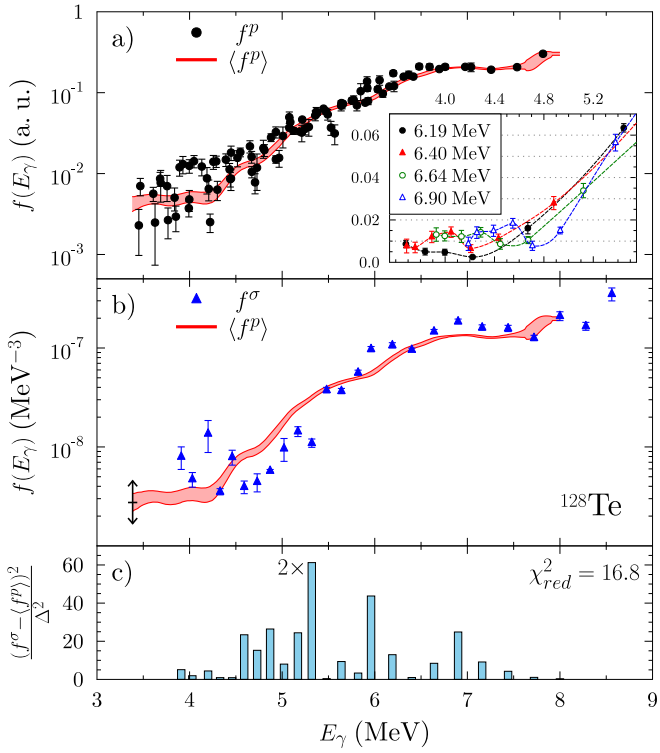

Fig. 2. Experimental results for ^{128}Te. **a**) All observed $f^p(E_\gamma)$ values extracted from primary transitions (black dots) from different excitation energies to different final states. The red shaded area corresponds to the external uncertainty of the Gaussian-weighted moving average of the data points. Inset of **a**) Single data sets from four different beam energies. **b**) Comparison of the two independently derived photon strength functions $f^p(E_\gamma)$ (from Fig. 2.a) and $f^\sigma(E_\gamma)$ (from photoabsorption cross section data). **c**) χ^2 analysis comparing both derived PSFs. For a detailed discussion see text.

of the combined data set. The inset of Fig. 2.a) exemplarily illustrates overlapping data points below $E_\gamma = 5.4$ MeV extracted from four different measurements with beam energies ranging from 6.19 MeV to 6.9 MeV. It is evident that the experimental data sets for different beam energies are not consistent with each other, i.e., they do not provide a unique shape for the derived PSF. The deviations between data sets with overlapping data points for $f^p_{exp}(E_\gamma)$ are as large as a factor of 2–3 and, thus, larger than can be explained by Porter–Thomas (PT) fluctuations [50] as discussed below. Therefore, it has to be concluded that for the given case of ^{128}Te the decay properties of the photo-excited states cannot be described by a single excitation-energy independent PSF, which contradicts the applicability of the BA hypothesis to the excitation energy range studied here.

The role of PT fluctuations is studied with a modified version of the Monte-Carlo-method based DICEBOX code [51] which simulates γ-ray cascades in NRF reactions. Based on the main input quantities such as the NLD and PSFs, random level schemes of an artificial nucleus are created taking PT fluctuations for the individual transition widths of each nuclear level into account. Then, several so-called nuclear realizations (in the present case 30) are generated. Each of these realizations has a different nuclear level schemes that, however, follows the same statistical properties defined by the NLD and PSFs. In the present case, the Back-Shifted Fermi Gas model is used for the NLD with the parameters $a = 13.04$ MeV^{-1} and $E_1 = 0.68$ MeV [52]. The PSF for the $E1$ contribution is determined from the measured photoabsorption cross section, while the parametrizations for the $M1$ and $E2$ contributions are taken from Ref. [53].

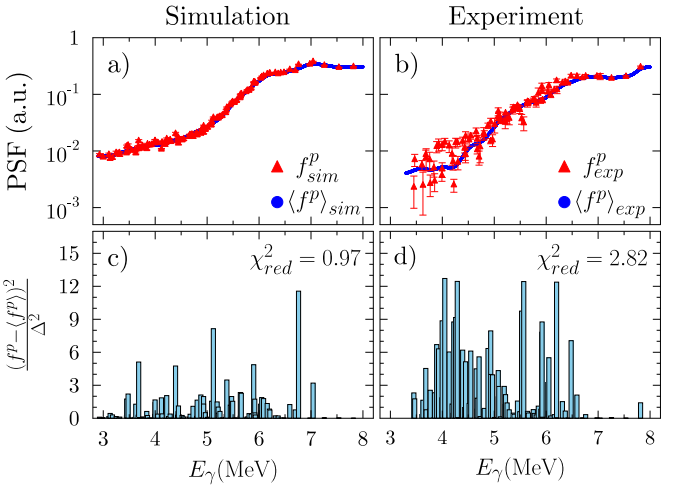

Fig. 3. Comparison of f^p extracted from DICEBOX simulations (**a**) to the experimental results (**b**). A χ^2 analysis is performed for each individual primary transition (red triangle) versus the moving average (blue dots) computed from all primary transitions for the simulation (**c**) and the experiment (**d**). The total error is defined as $\Delta^2 = (\Delta f^p)^2 + (\Delta_{PT})^2$ taking the statistical uncertainties (Δf^p) and PT fluctuations (Δ_{PT}) into account.

The γ-ray cascades for each realization generated with DICEBOX are analyzed in the same way as the experimental data to extract $f^p_{sim}(E_\gamma)$. Fig. 3.a) displays $f^p_{sim}(E_\gamma)$ values (red triangles) from one realization together with a moving average $\langle f^p \rangle_{sim}$ of the data points (blue dots) weighted by a Gaussian distribution of FWHM = 300 keV, which corresponds roughly to the spectral width of the photon beams produced at HIγS. Investigating the variation of the $f^p_{sim}(E_\gamma)$ values for all 30 realizations the effect of the PT fluctuations can be quantified by determining the standard deviation Δ_{PT} for each energy bin. In general for both, simulation and experiment, the deviations between individual $f^p_{sim/exp}$ and $\langle f^p \rangle_{sim/exp}$ can be expressed by

$$\chi^2_i = \frac{(f^p_{sim/exp,\,i} - \langle f^p \rangle_{sim/exp})^2}{\Delta^2_i} \,, \tag{2}$$

with $\Delta^2_i = (\Delta f^p_{sim/exp,\,i})^2 + (\Delta_{PT})^2$ (see Fig. 3.c). Here, $\Delta f^p_{sim/exp,\,i}$ is the statistical uncertainty of each data point. Since 10^5 cascades were simulated with DICEBOX the statistical uncertainties $\Delta f^p_{sim,\,i}$ are negligible in comparison to Δ_{PT}. Except for a few cases the deviations are small and result in an overall

$$\chi^2_{red} = \frac{1}{N-1} \cdot \sum_i \chi^2_i = 0.97 \tag{3}$$

As expected for the simulations the fluctuations of the f^p_{sim} values in Fig. 3.a) are in excellent statistical agreement with the computed moving average $\langle f^p \rangle_{sim}$ and originate from PT fluctuations.

Figs. 3.b) and d) show the corresponding results for the experimental data. In contrast to the DICEBOX simulations large fluctuations of the individual f^p_{exp} values in comparison to its moving average $\langle f^p \rangle_{exp}$ are observed in Fig. 3.b). These deviations are quantified in Fig. 3.d). The fluctuations of the experimental f^p_{exp} results are much more pronounced than observed in the simulation (see Fig. 3.c) despite taking statistical uncertainties Δf^p_{exp} as well as the simulated PT fluctuations Δ_{PT} into account. Moreover, the overall $\chi^2_{red} = 2.82$ indicates that the deviations cannot be explained by the statistical uncertainties and the expected PT fluctuations alone. The PT fluctuations would have to be a factor of

more than three larger in order to achieve a good agreement, i.e., $\chi^2_{red} \approx 1$.

In fact, the observed deviations may, in principle, be attributed to decay widths distributions that do not follow the PT distribution, but any other distribution. The validity of PT-distributed partial decay widths has been debated for many decades without any conclusive outcome so far (see, e.g., [54,55] and [56] for a recent review). Older studies show a good agreement of partial transition widths of neutron resonances with the PT distribution [50,57,58], while recent experimental data [59–63] and theoretical considerations discuss possibilities of non-statistical effects and modifications of the PT distribution [64,65]. The present data on ^{128}Te may indicate such deviations from PT fluctuations of partial γ-decay widths, however, the current experimental method is not sensitive to draw any conclusion on this issue.

Keeping the discussed deviations in mind, nevertheless the smoothed shape of the moving average of the experimental data $\langle f^p \rangle_{exp}$ is compared to $f^\sigma(E_\gamma)$ in Fig. 2.b). As a reminder, the method using the primary γ-ray transitions does only yield the E_γ dependence of $f^p_{exp}(E_\gamma)$ and, therefore, can be scaled freely (indicated by the black double-sided arrow) to the results for $f^\sigma(E_\gamma)$. In the present case, the scaling factor is chosen to minimize the deviations between $\langle f^p \rangle_{exp}$ and $f^\sigma(E_\gamma)$, where the individual

$$\chi^2_i = \frac{(f^\sigma_i - \langle f^p_{exp,\,i} \rangle)^2}{\Delta^2_i} \tag{4}$$

with $\Delta^2_i = (\Delta f^\sigma_i)^2 + (\Delta f^p_{exp,\,i})^2)$ are shown in Fig. 2.c). It is obvious, that the two shapes for both PSFs cannot be brought into a good agreement indicated by the overall minimized $\chi^2_{red} = 16.8$ [59–65].

5. Conclusion

In conclusion, the present results show that the decay properties of photo-excited states below the particle threshold in ^{128}Te ($S_n = 8.78$ MeV) cannot be described quantitatively within the ansatz of the statistical model. The results indicate that the BA hypothesis is not fulfilled for excitation energies between 4 MeV and 8 MeV in the case of ^{128}Te. A unique photon strength function consistent with the uncertainties of the measurement cannot be extracted. Deviations of a factor of two remain. For further conclusions to be drawn it is crucial to expand these experiments to other nuclei and conduct systematic studies on the equivalence of the PSF build on the ground state and excited states, respectively. The novel experimental approach presented in this work has proven to be suited for such studies.

Acknowledgements

The authors thank the HIγS accelerator group for providing ideal experimental conditions, V. Derya for her contribution to the γ^3 setup and M.N. Harakeh for stimulating discussions. This work was supported by the Alliance Program of the Helmholtz Association (HA216/EMMI), the Deutsche Forschungsgemeinschaft under Grant Nos. SFB 634 and ZI 510/7-1, and the U.S. Department of Energy, Office of Nuclear Physics, under Grant No. DE-FG02-97ER41033. The work of BL was supported by the GSI–TU Darmstadt cooperation agreement.

References

[1] D.M. Brink, Ph.D. thesis, Oxford University, 1955.
[2] P. Axel, Phys. Rev. 126 (1962) 671–683.
[3] J.A. Holmes, S.E. Woosley, W.A. Fowler, B.A. Zimmerman, At. Data Nucl. Data Tables 18 (1976) 305.
[4] S. Goriely, Phys. Lett. B 436 (1998) 10–18.
[5] F. Käppeler, R. Gallino, S. Bisterzo, W. Aoki, Rev. Mod. Phys. 83 (2011) 157–193.
[6] W. Hauser, H. Feshbach, Phys. Rev. A 87 (1952) 366.
[7] M. Herman, R. Capote, B. Carlson, P. Obložinský, M. Sin, A. Trkov, H. Wienke, V. Zerkin, Nucl. Data Sheets 108 (2007) 2655–2715, Special Issue on Evaluations of Neutron Cross Sections.
[8] A. Koning, Nuclear Data for Science and Technology, EDP Sciences, 2008.
[9] F. Sokolov, K. Fukuda, H.P. Nawada, IAEA TEC-DOC 1450, 2005.
[10] M. Salvatores, G. Palmiotti, Prog. Part. Nucl. Phys. 66 (2011) 144–166.
[11] International Atomic Energy Agency, Fission Product Yield Data for the Transmutation of Minor Actinide Nuclear Waste, 2008.
[12] M.N. Harakeh, A. van der Woude, Giant Resonances, Oxford University Press, 2001.
[13] D. Savran, T. Aumann, A. Zilges, Prog. Part. Nucl. Phys. 70 (2013) 210–245.
[14] C.T. Angell, S.L. Hammond, H.J. Karwowski, J.H. Kelley, M. Krtička, E. Kwan, A. Makinaga, G. Rusev, Phys. Rev. C 86 (2012), 051302(R).
[15] J. Isaak, D. Savran, M. Krtička, M. Ahmed, J. Beller, E. Fiori, J. Glorius, J. Kelley, B. Löher, N. Pietralla, C. Romig, G. Rusev, M. Scheck, L. Schnorrenberger, J. Silva, K. Sonnabend, A. Tonchev, W. Tornow, H. Weller, M. Zweidinger, Phys. Lett. B 727 (2013) 361–365.
[16] L. Netterdon, A. Endres, S. Goriely, J. Mayer, P. Scholz, M. Spieker, A. Zilges, Phys. Lett. B 744 (2015) 358–362.
[17] P.F. Bortignon, A. Bracco, R.A. Broglia, Giant Resonances: Nuclear Structure at Finite Temperature, Harwood Academic, Amsterdam, 1998.
[18] T. Koeling, Nucl. Phys. A 307 (1978) 139–162.
[19] M. Hussein, B. Carlson, L. Canto, Nucl. Phys. A 731 (2004) 163–174.
[20] G.W. Misch, G.M. Fuller, B.A. Brown, Phys. Rev. C 90 (2014) 065808.
[21] C.W. Johnson, Phys. Lett. B 750 (2015) 72–75.
[22] D. Rochman, S. Goriely, A. Koning, A. Ferroukhi, Phys. Lett. B 764 (2017) 109–113.
[23] G. Bartholomew, E. Earle, A. Ferguson, J. Knowles, M. Lone, Adv. Nucl. Phys. 7 (1973) 229–324.
[24] M. Stefanon, F. Corvi, Nucl. Phys. A 281 (1977) 240–260.
[25] S. Raman, O. Shahal, G.G. Slaughter, Phys. Rev. C 23 (1981) 2794–2797.
[26] J. Kopecky, M. Uhl, Phys. Rev. C 41 (1990) 1941–1955.
[27] M. Krtička, F. Bečvář, J. Honzátko, I. Tomandl, M. Heil, F. Käppeler, R. Reifarth, F. Voss, K. Wisshak, Phys. Rev. Lett. 92 (2004) 172501.
[28] A.C. Larsen, S. Goriely, Phys. Rev. C 82 (2010) 014318.
[29] M. Wiedeking, L.A. Bernstein, M. Krtička, D.L. Bleuel, J.M. Allmond, M.S. Basunia, J.T. Burke, P. Fallon, R.B. Firestone, B.L. Goldblum, R. Hatarik, P.T. Lake, I.-Y. Lee, S.R. Lesher, S. Paschalis, M. Petri, L. Phair, N.D. Scielzo, Phys. Rev. Lett. 108 (2012) 162503.
[30] R. Massarczyk, R. Schwengner, F. Dönau, S. Frauendorf, M. Anders, D. Bemmerer, R. Beyer, C. Bhatia, E. Birgersson, M. Butterling, Z. Elekes, A. Ferrari, M.E. Gooden, R. Hannaske, A.R. Junghans, M. Kempe, J.H. Kelley, T. Kögler, A. Matic, M.L. Menzel, S. Müller, T.P. Reinhardt, M. Röder, G. Rusev, K.D. Schilling, K. Schmidt, G. Schramm, A.P. Tonchev, W. Tornow, A. Wagner, Phys. Rev. Lett. 112 (2014) 072501.
[31] M. Guttormsen, A.C. Larsen, A. Görgen, T. Renstrøm, S. Siem, T.G. Tornyi, G.M. Tveten, Phys. Rev. Lett. 116 (2016) 012502.
[32] J. Kopecky, S. Goriely, S. Péru, S. Hilaire, M. Martini, Phys. Rev. C 95 (2017) 054317.
[33] D. Martin, P. von Neumann-Cosel, A. Tamii, N. Aoi, S. Bassauer, C.A. Bertulani, J. Carter, L. Donaldson, H. Fujita, Y. Fujita, T. Hashimoto, K. Hatanaka, T. Ito, A. Krugmann, B. Liu, Y. Maeda, K. Miki, R. Neveling, N. Pietralla, I. Poltoratska, V.Y. Ponomarev, A. Richter, T. Shima, T. Yamamoto, M. Zweidinger, Phys. Rev. Lett. 119 (2017) 182503.
[34] R. Schwengner, G. Rusev, N. Tsoneva, N. Benouaret, R. Beyer, M. Erhard, E. Grosse, A.R. Junghans, J. Klug, K. Kosev, H. Lenske, C. Nair, K.D. Schilling, A. Wagner, Phys. Rev. C 78 (2008) 064314.
[35] R. Massarczyk, R. Schwengner, F. Dönau, E. Litvinova, G. Rusev, R. Beyer, R. Hannaske, A.R. Junghans, M. Kempe, J.H. Kelley, T. Kögler, K. Kosev, E. Kwan, M. Marta, A. Matic, C. Nair, R. Raut, K.D. Schilling, G. Schramm, D. Stach, A.P. Tonchev, W. Tornow, E. Trompler, A. Wagner, D. Yakorev, Phys. Rev. C 86 (2012) 014319.
[36] C. Romig, J. Beller, J. Glorius, J. Isaak, J.H. Kelley, E. Kwan, N. Pietralla, V.Y. Ponomarev, A. Sauerwein, D. Savran, M. Scheck, L. Schnorrenberger, K. Sonnabend, A.P. Tonchev, W. Tornow, H.R. Weller, A. Zilges, M. Zweidinger, Phys. Rev. C 88 (2013) 044331.
[37] L. Henden, L. Bergholt, M. Guttormsen, J. Rekstad, T.S. Tveter, Nucl. Phys. A 589 (1995) 249–266.
[38] A. Schiller, L. Bergholt, M. Guttormsen, E. Melby, J. Rekstad, S. Siem, Nucl. Instrum. Methods Phys. Res., Sect. A, Accel. Spectrom. Detect. Assoc. Equip. 447 (2000) 498–511.
[39] R. Schwengner, S. Frauendorf, A.C. Larsen, Phys. Rev. Lett. 111 (2013) 232504.
[40] F. Bečvář, J. Honzátko, M. Krtička, S. Pašić, I. Tomandl, Nucl. Instrum. Methods Phys. Res., Sect. B, Beam Interact. Mater. Atoms 261 (2007) 930–933.

[41] J.L. Ullmann, T. Kawano, T.A. Bredeweg, A. Couture, R.C. Haight, M. Jandel, J.M. O'Donnell, R.S. Rundberg, D.J. Vieira, J.B. Wilhelmy, J.A. Becker, A. Chyzh, C.Y. Wu, B. Baramsai, G.E. Mitchell, M. Krtička, Phys. Rev. C 89 (2014) 034603.
[42] U. Kneissl, H.H. Pitz, A. Zilges, Prog. Part. Nucl. Phys. 37 (1996) 349–433.
[43] B. Löher, Probing the Decay Characteristics of the Pygmy Dipole Resonance in the Semi-Magic Nucleus ^{140}Ce with γ–γ Coincidence Measurements, Ph.D. thesis, Johannes Gutenberg-Universität Mainz, 2014, https://publications.ub.uni-mainz.de/theses/volltexte/2014/3819/pdf/3819.pdf.
[44] J. Isaak, Investigation of Decay Properties of the Pygmy Dipole Resonance and Photon Strength Functions on Excited States in $(\vec{\gamma}, \gamma'\gamma'')$ Reactions, Ph.D. thesis, Johannes Gutenberg-Universität Mainz, 2016, https://publications.ub.uni-mainz.de/theses/volltexte/2016/100000664/pdf/100000664.pdf.
[45] A.P. Tonchev, S.L. Hammond, J.H. Kelley, E. Kwan, H. Lenske, G. Rusev, W. Tornow, N. Tsoneva, Phys. Rev. Lett. 104 (2010) 072501.
[46] P.M. Goddard, N. Cooper, V. Werner, G. Rusev, P.D. Stevenson, A. Rios, C. Bernards, A. Chakraborty, B.P. Crider, J. Glorius, R.S. Ilieva, J.H. Kelley, E. Kwan, E.E. Peters, N. Pietralla, R. Raut, C. Romig, D. Savran, L. Schnorrenberger, M.K. Smith, K. Sonnabend, A.P. Tonchev, W. Tornow, S.W. Yates, Phys. Rev. C 88 (2013) 064308.
[47] B. Löher, D. Savran, T. Aumann, J. Beller, M. Bhike, N. Cooper, V. Derya, M. Duchêne, J. Endres, A. Hennig, P. Humby, J. Isaak, J. Kelley, M. Knörzer, N. Pietralla, V. Ponomarev, C. Romig, M. Scheck, H. Scheit, J. Silva, A. Tonchev, W. Tornow, F. Wamers, H. Weller, V. Werner, A. Zilges, Phys. Lett. B 756 (2016) 72–76.
[48] B. Löher, V. Derya, T. Aumann, J. Beller, N. Cooper, M. Duchêne, J. Endres, E. Fiori, J. Isaak, J. Kelley, M. Knörzer, N. Pietralla, C. Romig, D. Savran, M. Scheck, H. Scheit, J. Silva, A. Tonchev, W. Tornow, H. Weller, V. Werner, A. Zilges, Nucl. Instrum. Methods Phys. Res., Sect. A, Accel. Spectrom. Detect. Assoc. Equip. 723 (2013) 136–142.
[49] H.R. Weller, M.W. Ahmed, H. Gao, W. Tornow, Y.K. Wu, M. Gai, R. Miskimen, Prog. Part. Nucl. Phys. 62 (2009) 257–303.
[50] C.E. Porter, R.G. Thomas, Phys. Rev. 104 (1956) 483–491.
[51] F. Bečvář, Nucl. Instrum. Methods Phys. Res., Sect. A, Accel. Spectrom. Detect. Assoc. Equip. 417 (1998) 434–449.
[52] T. von Egidy, D. Bucurescu, Phys. Rev. C 80 (2009) 054310.
[53] T. Belgya, O. Bersillon, R. Capote, T. Fukahori, G. Zhigang, S. Goriely, M. Herman, A.V. Ignatyuk, S. Kailas, A. Koning, P. Obložinský, V. Plujko, P. Young, Handbook for Calculations of Nuclear Reaction Data, RIPL-2, IAEA-TECDOC, vol. 1506, IAEA, Vienna, 2006.
[54] C.E. Porter, Statistical Theories of Spectra, Academic, New York, 1965.
[55] T.A. Brody, J. Flores, J.B. French, P.A. Mello, A. Pandey, S.S.M. Wong, Rev. Mod. Phys. 53 (1981) 385–479.
[56] H.A. Weidenmüller, G.E. Mitchell, Rev. Mod. Phys. 81 (2009) 539–589.
[57] R.U. Haq, A. Pandey, O. Bohigas, Phys. Rev. Lett. 48 (1982) 1086–1089.
[58] O. Bohigas, R.U. Haq, A. Pandey, in: K.H. Bockhoff (Ed.), Nuclear Data for Science and Technology, Reidel, Dordrecht, 1983, p. 809.
[59] A. Adams, G. Mitchell, J.J.F. Shriner, Phys. Lett. B 422 (1998) 13–18.
[60] J.F. Shriner, C.A. Grossmann, G.E. Mitchell, Phys. Rev. C 62 (2000) 054305.
[61] P.E. Koehler, F. Bečvář, M. Krtička, J.A. Harvey, K.H. Guber, Phys. Rev. Lett. 105 (2010) 072502.
[62] P.E. Koehler, Phys. Rev. C 84 (2011) 034312.
[63] P.E. Koehler, A.C. Larsen, M. Guttormsen, S. Siem, K.H. Guber, Phys. Rev. C 88 (2013) 041305.
[64] A. Volya, H.A. Weidenmüller, V. Zelevinsky, Phys. Rev. Lett. 115 (2015) 052501.
[65] E. Bogomolny, Phys. Rev. Lett. 118 (2017) 022501.